Tunable Low-Jitter Low-Drift Spurious-Free Transposed-Frequency Optoelectronic Oscillator

S. Esmail Hosseini, *Graduate Student Member, IEEE*, Ali Banai, *Member, IEEE*, and Franz X. Kärtner, *Fellow, IEEE*

***Abstract*— We propose and theoretically and experimentally demonstrate a novel tunable spurious-free single-loop optoelectronic oscillator (OEO) with low drift and low-phase noise. In the proposed transposed-frequency OEO (TF-OEO), a nonreciprocal bias unit and an optical phase modulator in a fiber Sagnac interferometer function jointly as an intrinsically drift-free intensity modulator, which improves the long-term drift. Besides, a transposed-frequency low-noise filtered amplifier is used which replaces the conventional radio frequency (RF) bandpass filter (BPF) and RF amplifier with an intermediate frequency (IF) BPF, an ultralow phase noise IF amplifier, and a tunable local oscillator, to attain frequency tuning and single-frequency selection with ultralow phase noise at the same time. The quality of the generated microwave signals is theoretically investigated and verified by experiments. Preliminary phase noise, frequency stability, spurious noise levels, and frequency tunability of the photonically generated microwave signal are also investigated. A microwave signal with a frequency tunable range of 15 MHz around 10.833 GHz is generated with no spurs. The generated microwave oscillation has a single-sideband phase noise of −120 dBc/Hz at 10 kHz offset from 10.833 GHz carrier, with 36 fs RMS timing jitter integrated from 1 kHz to 10 MHz. Long-term frequency stability measurements show ±0.05 ppm maximum fractional frequency deviation over 60 h, which is mainly limited by drift of the fiber delay line. The measured results show the long-term frequency stability (in terms of overlapping Allan deviation) within 8.7×10^{-9} at 1000 s averaging time.**

***Index Terms*— Long-term stability, optoelectronic oscillators (OEOs), Sagnac loop, spurious free, transposed frequency.**

I. Introduction

ULTRALOW phase noise microwave oscillators with high stability are required for many applications such as high-performance radar systems [1], large-scale high-precision remote synchronization (such as in free-electron lasers) [2], [3], navigation, communication, and signal measurement instrumentations. With recent advances, various types of ultrapure microwave oscillators have been developed, which culminated in the state-of-the-art ultrapure microwave oscillators such as sapphire-loaded cavity oscillators [4], [5], photonic generation of microwave oscillations from stabilized femtosecond mode-locked lasers [2], [3], [6], and optoelectronic oscillators (OEOs) [7], [8].

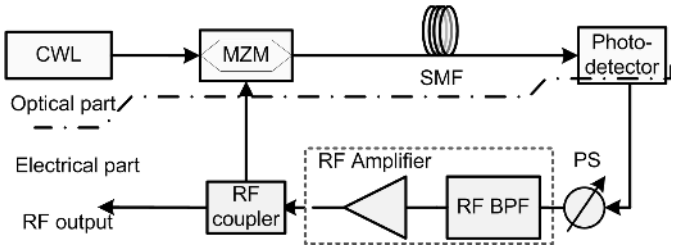

Fig. 1. Basic architecture of the conventional OEO. CWL: continuous wave laser. SMF: single mode fiber.

An OEO is a delay-line oscillator that utilizes a very long low-loss optical fiber as a high-Q cavity. The most basic architecture of an OEO is shown in Fig. 1. The Q-factor of such a delay-line oscillator is approximately equal to $Q = 2\pi f \tau$ [7], where f is the frequency of oscillation of the oscillator and τ is the total time delay in the oscillator loop. A simple solution to reach ultralow phase noise OEOs is to use a long fiber loop line. However, the long delay line causes equally spaced spurious in the output spectrum of the oscillator. One way to alleviate this unwanted spurs is using a bandpass filter (BPF) in the microwave section of the loop. The spacing between these spurs is inversely proportioned to the length of delay line. As an example, for a 4 Km fiber, this spacing is 50 kHz and it is too difficult to reject sufficiently the unwanted spurs. Consider a narrow-band BPF at 10 GHz with 20 MHz bandwidth. There will be 400 spurious oscillating modes pass through this filter. In many applications, existence of such huge number of spurs near the main oscillation mode is unacceptable. Many techniques have been proposed for reducing the amplitude of the unwanted cavity modes such as using multiple loops in an OEO [9]–[19], dual injection-locked OEO [20]–[23], and coupled OEO [24]–[27]. However, by using these configurations not only are the spurious modes not completely eliminated but also the phase noise degrades relative to the single-loop OEO with long-fiber because the overall Q-factor is averaged between the short and long loops [20].

Besides, most of the previous OEO demonstrations are based on a Mach–Zehnder modulator (MZM), while the bias point of the MZM is environmentally sensitive and drifts during the operation, which is not desired when long-term stability is required for ultralow phase noise photonic microwave generation. Hence, for a long-term operation of

Manuscript received October 1, 2015; revised December 14, 2015, June 24, 2016, August 13, 2016, and December 21, 2016; accepted December 22, 2016.

S. E. Hosseini is with the Department of Electrical and Computer Engineering, Shiraz University, Shiraz 71946-84471, Iran (e-mail: se.hosseini@shirazu.ac.ir).

A. Banai is with the Department of Electrical Engineering, Sharif University of Technology, Tehran 11155-4363, Iran (e-mail: banai@sharif.edu).

F. X. Kärtner is with the Center for Free Electron Laser Science, CFEL at DESY and University of Hamburg, D-22607 Hamburg, Germany, and also with the Department of Electrical Engineering and Research Laboratory of Electronics, Massachusetts Institute of Technology, Cambridge MA 02139 USA (e-mail: franz.kaertner@desy.de).

Color versions of one or more of the figures in this paper are available online at http://ieeexplore.ieee.org.

Digital Object Identifier 10.1109/TMTT.2016.2646681

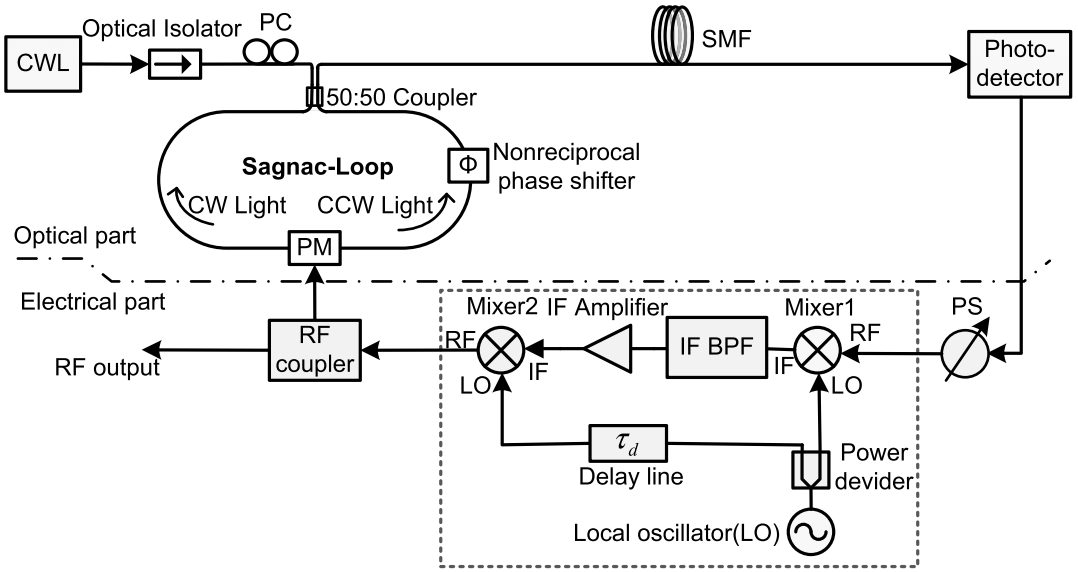

Fig. 2. Schematic illustration of the Sagnac-loop-based TF-OEO. PC: polarization controller.

an OEO with MZM, an automatic feedback bias control and tracking is necessary so as to lock the selected operating bias point.

In [28]–[36], a technique to achieve a bias-drift free OEO based on a phase modulator combined with a dispersive device was proposed. In the proposed structure, the dispersive device converts phase-modulation into intensity-modulation (PM-IM). In this structure, a dispersive device such as a fiber Bragg grating is required for PM-IM conversion. This is because a photodetector acts as an amplitude detector. A signal with phase modulation has a constant amplitude, so if it is directly put on a photodetector no modulating signal will be detected except a dc.

In previous work, we proposed and experimentally showed an architecture for an OEO based on a PM in a fiber Sagnac interferometer [37]. Because no bias is necessary for a PM, the bias drifting problems associated with the MZM are automatically removed so that the Sagnac-loop based OEO will be intrinsically bias-drift free. A more detailed discussion of the Sagnac-loop based OEO is found in [37].

It is also well known in the literature that the near-carrier phase noise of OEOs is determined by the flicker noise of the radio frequency (RF) amplifiers in the loop [38]–[42]. So in order to have ultralow phase noise OEO, we have to use RF amplifiers with low flicker noise.

Although many techniques have been proposed to improve the frequency stability, phase noise, spur levels, and tunability of the generated microwave oscillation, to the best of our knowledge, no methods have been proposed to address all these problems at the same time. In this paper, a novel single-loop OEO is introduced in which the conventional MZM and RF filtered amplifiers are replaced with a PM in a Sagnac loop and TF-LNFA, respectively, to achieve a tunable, spurious-free, low-drift, low phase noise OEO.

With the proposed transposed-frequency OEO (TF-OEO), a microwave oscillation at 10.833 GHz frequency is generated and its preliminary phase noise, frequency stability, spurs, and tunability performances are investigated in Section IV. A theoretical model is also presented in Section III to study the performance of the proposed TF-OEO, which is also verified by the experiments.

II. Transposed-Frequency OEO: A Novel Architecture

A block diagram of the proposed Sagnac-loop-based TF-OEO is shown in Fig. 2. As shown in this figure, the conventional RF BPF and RF amplifier (as shown in the dashed-line box in Fig. 1) are replaced with a TF-LNFA (as shown in the dashed-line box in Fig. 2). Also, the MZM is replaced with a fiber Sagnac interferometer incorporating a PM and a nonreciprocal bias unit.

A more detailed discussion on the performance of the TF-OEO is presented in the following sections.

A. Improving Long-Term Drift

The significant feature of the proposed TF-OEO is that the modulator does not require a bias, so bias drifting problems associated with the conventional OEO due to the MZM are automatically removed. In addition, there is no need of an automatic feedback bias control and tracking, which greatly simplifies the implementation. A more detailed discussion is found in [37].

It is worth mentioning here that the optical fiber length fluctuations are the other sources of drift in OEOs [43], [44]. Several techniques have already been proposed to compensate the drift in the fiber lengths [14], [45]–[49].

B. Eliminating Spurs and Improving Phase Noise

As we have already mentioned, the RF amplifier flicker noise is the limiting factor of the OEO close-to-carrier

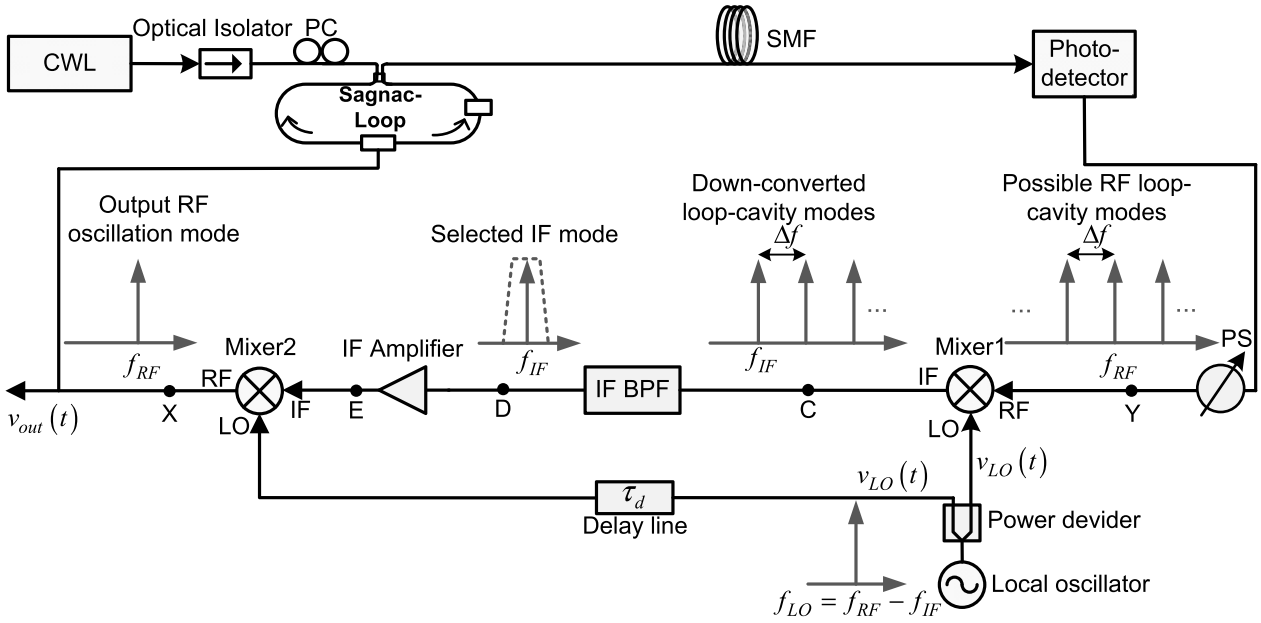

Fig. 3. Illustration of the TF-OEO single mode oscillation.

phase noise. Several techniques have been developed to reduce the microwave amplifiers flicker noise for use in a microwave oscillator, such as feedforward amplifiers [50]–[52], feedback amplifiers [51], [53], parallel amplifiers [54], and transposed-gain amplifiers (TGA) [53], [55].

Driscoll and Weinert [53] and Everard and Page-Jones [55] proposed, independently, the TGA as a low flicker noise amplifier. The TGA uses HF/VHF silicon bipolar junction transistor (Si BJT) instead of microwave GaAs transistors. It is well known that HF/VHF Si BJTs and Si-based mixers have lower flicker noise than microwave GaAs transistors [54], [56]. Flicker noise levels of microwave GaAs amplifiers are typically 30 dB higher than that of the HF/VHF Si BJTs and 20 dB higher than that of the silicon-based mixers [57]–[59].

In this amplifier, the amplification is provided at a lower frequency than the oscillator output frequency by downconverting the microwave frequency to an intermediate frequency (IF) using an LO and upconverting back to the primary frequency at the output. Some very low noise microwave oscillators were built using TGA [53], [55], [60]. The level of phase noise suppression is of the order of 20–30 dB at offsets around 10 kHz [53], [55], [56], [60]. A more detailed discussion on the TF-OEO phase noise can be found in Section III-A.

In the conventional TGA [53], [55] there is no IF BPF in the structure but here, we insert a narrow-band IF BPF (crystal filter) in the IF part to select one of the downconverted loop cavity modes and effectively suppress other modes as long as the IF BPF bandwidth (B is of the order of a few kHz) is lower than the free-spectral range (FSR of the order of a few ten kHz), $B <$ FSR. So using this structure the OEO will operate in a single mode. In addition, the overall Q-factor of the loop is maintained and the phase noise does not increase compared to that of the conventional OEO. Besides, it allows using a longer length fiber loop to reduce further the OEO phase noise without the need of ultranarrow-band RF BPF in the loop.

Besides, there is no initial noise-dependent transient selective mode competition process in the loop because only one loop cavity mode falls in the passband of the IF BPF that satisfies the Barkhausen criterion, i.e., the loop gain must be unity. As a consequence, there is no ambiguity of oscillation frequency and there is also no need of a slow switch-ON procedure to obtain a single mode operation that is needed when an RF BPF (that hundreds of loop cavity modes fall within its bandwidth) is used [61]. In addition, there is only one oscillating mode and so the mode-hopping phenomena, arising from noise and drift in center frequency of the non-stabilized RF BPF, is prevented which is expected to occur in the conventional OEO because possible loop cavity modes are falling within the bandwidth of the RF BPF [42].

Hence, the TF-OEO is a microwave/millimeter-wave oscillator where the signal amplification and mode selecting portion are operating at an HF/VHF frequency. It is worth mentioning here that, we know that silicon germanium heterojunction bipolar transistors (SiGe HBT) are another technology with high frequency operation and low noise characteristics but we proposed HF/VHF Si BJT in the TF-LNFA to eliminate spurs and reduce phase noise simultaneously.

C. Frequency Tunability

The microwave signal is downconverted and upconverted using the same LO having a frequency $f_{\mathrm{LO}} = f_{\mathrm{RF}} - f_{\mathrm{IF}}$ (as shown in Fig. 3). The same delay as that of the IF path is used in the LO path by inserting a delay line (τ_d) in the LO path, in order to ensure that the LO phase noise does not degrade that of the OEO. So there is no need to have an ultrapure LO.

On the other hand, in order to output microwave oscillation that is not sensitive to the instability of the LO, its frequency uncertainty (δf_{LO}) should be less than $B/2$. Thus as the frequency of the LO varies, the frequency of the IF portion of the loop varies inversely so that the microwave output

frequency of the TF-OEO does not change. So in addition to the no need of an ultrapure LO, there is also no need of an ultrastable LO. Hence, it permits the use of a low-cost low phase noise unstabilized LO.

Finally, the condition on the bandwidth of the IF BPF to ensure the single mode operation and also the insensitivity of the microwave oscillation frequency to the instability of the LO, can be expressed as $2\delta f_{\mathrm{LO}} < B < \mathrm{FSR}$.

In general, the output of mixer2 (in Fig. 3) contains two components $f_{\mathrm{RF}} = f_{\mathrm{LO}} + f_{\mathrm{IF}}$ and $f_{\mathrm{image}} = f_{\mathrm{LO}} - f_{\mathrm{IF}}$. In order to have a sustained oscillation at f_{RF} in the steady state it must be one of the loop cavity modes so

$$f_{\mathrm{RF}} = m_1 \mathrm{FSR} \tag{1}$$

where m_1 is a nonnegative integer. In addition, to have no oscillation at the image frequency, it must not be a loop cavity mode, that is

$$f_{\mathrm{image}} = f_{\mathrm{LO}} - f_{\mathrm{IF}} = f_{\mathrm{RF}} - 2f_{\mathrm{IF}} \neq m_2 \mathrm{FSR} \tag{2}$$

where m_2 is an integer. Using (1) and (2), we find that the center frequency of the IF portion of the loop and LO frequency must satisfy the conditions

$$f_{\mathrm{LO}} \neq (m_3/2)\mathrm{FSR} \tag{3}$$

$$f_{\mathrm{IF}} \neq (m_4/2)\mathrm{FSR} \tag{4}$$

where m_3 and m_4 are integers. We know that the above two conditions are the same and if one of them satisfies, the other will satisfy too. Otherwise, if $f_{\mathrm{IF}} = m_4\mathrm{FSR}/2$ then the image frequency will fall on a loop cavity mode position and will oscillate, so in order to suppress it effectively, an RF BPF whose bandwidth is less than $2f_{\mathrm{IF}}$ must be used after mixer2.

In this scheme, by tuning the frequency of the LO, the frequency of the OEO can be tuned, which would not change continuously but would jump between loop cavity modes. So the frequency tuning step (tuning resolution) is the FSR of the OEO loop that is of the order of a few tens of kilohertz for a few kilometers' fiber loop length. For smaller tuning steps, longer fiber loops must be used, which is possible as long as we use an IF BPF as a selecting mode filter.

For fine-tuning, we can use a phase shifter (PS) after mixer2 in the OEO loop. Thus tuning of the TF-OEO can be either discrete coarse or continuous fine. Discrete coarse tuning with tuning resolution of the order of the FSR (a few tens of kilohertz) can be realized by tuning the frequency of the LO and continuous fine-tuning can be realized by adjusting the PS. The tuning range and tuning speed of the TF-OEO is limited by the RF BPF bandwidth and tuning speed of the PS, respectively, in the fine-tuning case and by those of the LO in the coarse tuning case. So using TF-OEO, frequency tuning with no mode hopping and with fast tuning speed and low tuning resolution can be obtained.

III. Theory, Results, and Discussion

Fig. 3 shows a detailed diagram of the proposed TF-OEO chosen for analysis. We assume that the microwave signal around the loop will be a sinusoidal wave with angular frequency ω_{RF}, amplitude V_{RF}, and phase β which is

$$v_{\mathrm{out}}(t) = V_{\mathrm{RF}} \cos(\omega_{\mathrm{RF}} t + \beta). \tag{5}$$

That is the input RF voltage applied to the RF input port of the PM. The electric voltage at the output of the photodetector (point Y in Fig.3) can be expressed as [37]

$$v_Y(t) = V_{\mathrm{ph}}[1 - \cos(\pi v_{\mathrm{out}}(t - \tau_L)/V_{\pi,\mathrm{for}} + \Phi)] \tag{6}$$

where Φ is the phase difference between clockwise (CW) and counterclockwise (CCW) propagating light caused by the bias unit, $V_{\pi,\mathrm{for}}$ is the half-wave voltage of the PM for the CW (forward) propagating light, V_{ph} is the photodetector voltage defined as $V_{\mathrm{ph}} = (1 - L)P_{\mathrm{in}}\rho R/2$, where L is the Sagnac loop loss, P_{in} is the laser power into the Sagnac loop, R is the load impedance of the photodetector and ρ is its responsivity and $\tau_L = nL/c$ is the time delay of the fiber loop, where L is the length of the optical fiber, n is its refraction index, and c is the velocity of light in the free space. We assume in our analysis that all components are working linearly except the PM which is saturated and limits the amplitude of oscillation.

By substituting (5) into (6) and using the Jacobi-Anger expansion [62]

$$e^{iz\cos\alpha} = \sum_{n=-\infty}^{+\infty} i^n J_n(z) e^{in\alpha} \tag{7}$$

where J_n is the nth order Bessel function of the first kind, using $J_{-n}(z) = (-1)^n J_n(z)$, (6) can be written as

$$v_Y(t) = V_{\mathrm{ph}}\left[1 - 2\sum_{n=0}^{+\infty}(-1)^n J_{2n+1}(\pi V_{\mathrm{RF}}/V_\pi) \times \cos((2n+1)\omega_{\mathrm{RF}}(t-\tau_L) + (2n+1)\beta)\right]. \tag{8}$$

Here we assume that $\Phi = \pi/2$ in order to have the highest small-signal gain (a more detailed discussion is found in [37]).

It is clear from (8) that the output voltage of the photodetector consists of the fundamental frequency and its harmonic components located in different regions of the spectrum, the so-called zero zone (at low frequencies), first or fundamental zone (in the vicinity of the input frequency range), and higher order zones (in the vicinity of the harmonics of the fundamental) [63].

We assume that the signal of the LO after the equal power divider is

$$v_{\mathrm{LO}}(t) = V_{\mathrm{LO}} \cos(\omega_{\mathrm{LO}} t + \varphi_{\mathrm{LO}}(t)). \tag{9}$$

The downconverted signal can be obtained from (8) and (9) as

$$\begin{aligned} v_C(t) = {} & \sqrt{C_m} V_{\mathrm{ph}} V_{\mathrm{LO}} \cos(\omega_{\mathrm{LO}} t + \varphi_{\mathrm{LO}}(t)) \\ & - \sqrt{C_m} V_{\mathrm{ph}} V_{\mathrm{LO}} \sum_{n=0}^{+\infty}(-1)^n J_{2n+1}(\pi V_{\mathrm{RF}}/V_\pi) \\ & \times \cos((2n+1)\omega_{\mathrm{RF}}(t-\tau_L) + (2n+1) \\ & \times \beta - \varphi_m - \omega_{\mathrm{LO}} t - \varphi_{\mathrm{LO}}(t)) \\ & - \sqrt{C_m} V_{\mathrm{ph}} V_{\mathrm{LO}} \sum_{n=0}^{+\infty}(-1)^n J_{2n+1}(\pi V_{\mathrm{RF}}/V_\pi) \\ & \times \cos((2n+1)\omega_{\mathrm{RF}}(t-\tau_L) + (2n+1) \\ & \times \beta - \varphi_m + \omega_{\mathrm{LO}} t + \varphi_{\mathrm{LO}}(t)) \end{aligned} \tag{10}$$

where C_m is the mixer conversion loss and φ_m is the phase shift due to the mixer.

The IF BPF is assumed as a general BPF with the following transfer function:

$$H(\omega_{\rm IF}) = H_0/(1 + jQ(\omega_{\rm IF}/\omega_n - \omega_n/\omega_{\rm IF})) \tag{11}$$

where $\omega_{\rm IF} = \omega_{\rm RF} - \omega_{\rm LO}$ is the angular frequency of the IF section, Q is the IF BPF quality factor, and ω_n is its center frequency. If $\omega_{\rm IF} + \omega_n \simeq 2\omega_{\rm IF}$ and $\omega_{\rm IF} - \omega_n \ll \omega_n/2Q$ (that is realistic because the center frequency of the IF BPF needs to be close to the downconverted oscillation frequency), (11) can be approximated as

$$H(\omega_{\rm IF}) \simeq H_0 e^{-j\tau_{\rm IF}(\omega_{\rm IF}-\omega_n)} \tag{12}$$

where $\tau_{\rm IF} = 2Q/\omega_n$ is the group delay of the IF BPF at $\omega_{\rm IF} = \omega_n$. So v_C is attenuated by H_0 and phase shifted by $\tau_{\rm IF}(\omega_{\rm IF} - \omega_n)$. Also, phase transfer function of a general BPF can be expressed as [54]

$$B(s) = \frac{1}{\tau_{\rm IF}} \frac{s + 1/\tau_{\rm IF} + \Omega^2\tau_{\rm IF}}{(s + 1/\tau_{\rm IF} - j\Omega)(s + 1/\tau_{\rm IF} + j\Omega)} \tag{13}$$

where $\Omega = \omega_{\rm IF} - \omega_n$. If $\Omega \ll \omega_n/2Q$ and $\omega\tau_{\rm IF} \ll 1$, (13) can be approximated as

$$B(\omega) \simeq e^{-j\omega\tau_{\rm IF}}. \tag{14}$$

So the phase of the LO is delayed at the output of the IF BPF with a value equal to $\tau_{\rm IF}$.

At the output of the IF BPF, the fundamental harmonic is selected and all other harmonics are attenuated due to the passband behavior of the TF-LNFA around the fundamental harmonic. So the output signal of the IF BPF is obtained from (10) as

$$\begin{aligned} v_D(t) = {} & H_0\sqrt{C_m}V_{\rm ph}V_{\rm LO}J_1(\pi V_{\rm RF}/V_\pi) \\ & \times \cos(\omega_{\rm IF}t - \omega_{\rm RF}\tau_L - \varphi_m - \tau_{\rm IF}(\omega_{\rm IF} - \omega_n) \\ & + \beta - \varphi_{\rm LO}(t - \tau_{\rm IF})). \end{aligned} \tag{15}$$

Transfer function of the IF amplifiers is assumed as

$$H_a(\omega) \simeq G_a e^{-j\varphi_a} \tag{16}$$

where G_a is the amplifier voltage gain, so its output signal can be expressed as

$$\begin{aligned} v_E(t) = {} & G_a H_0\sqrt{C_m}V_{\rm ph}V_{\rm LO}J_1(\pi V_{\rm RF}/V_\pi) \\ & \times \cos(\omega_{\rm IF}t - \omega_{\rm RF}\tau_L - \varphi_m - \tau_{\rm IF}(\omega_{\rm IF} - \omega_n) \\ & + \beta - \varphi_a - \varphi_{\rm LO}(t - \tau_{\rm IF})). \end{aligned} \tag{17}$$

That is upconverted by the mixer2 so voltage at point X in Fig. 3 is

$$\begin{aligned} v_X(t) = {} & G_L V_{\rm RF}\cos(\omega_{\rm RF}t - \omega_{\rm RF}\tau_L - 2\varphi_m - \varphi_a + \beta \\ & - \tau_{\rm IF}(\omega_{\rm IF} - \omega_n) - \varphi_{\rm LO}(t - \tau_{\rm IF})\varphi_{\rm LO}(t - \tau_d)) \\ & + G_L V_{\rm RF}\cos((2\omega_{\rm LO} - \omega_{\rm RF})t + \omega_{\rm RF}\tau_L + 2\varphi_m + \varphi_a \\ & - \beta + \tau_{\rm IF}(\omega_{\rm IF} - \omega_n) + \varphi_{\rm LO}(t - \tau_{\rm IF}) + \varphi_{\rm LO}(t - \tau_d)) \end{aligned} \tag{18}$$

where $G_L = G_a H_0 C_m V_{\rm ph} V_{\rm LO} J_1(\pi V_{\rm RF}/V_\pi)/V_{\rm RF}$ is the voltage gain of the fundamental harmonic and where τ_d is the time delay in the parallel path from the LO. As already mentioned, if $\omega_{\rm IF}$ satisfies (4), $\omega_{\rm image}$ would not be a possible loop-cavity mode so it is eliminated, therefore

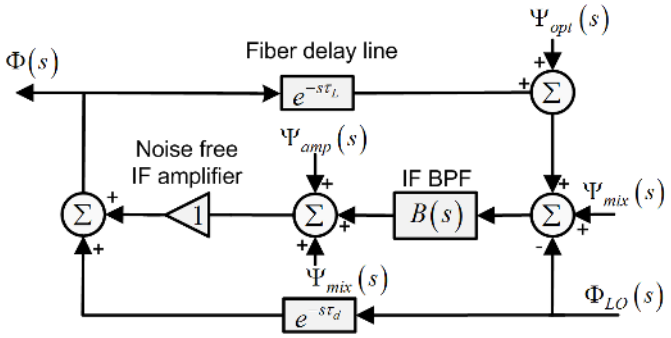

Fig. 4. Phase-space model for the proposed Sagnac-loop-based TF-OEO.

$$\begin{aligned} v_X(t) = {} & G_L V_{\rm RF}\cos(\omega_{\rm RF}t - \omega_{\rm RF}\tau_L - 2\varphi_m - \varphi_a + \beta \\ & - \tau_{\rm IF}(\omega_{\rm IF} - \omega_n) - \varphi_{\rm LO}(t - \tau_{\rm IF}) + \varphi_{\rm LO}(t - \tau_d)). \end{aligned} \tag{19}$$

If τ_d is adjusted such that $\tau_d = \tau_{\rm IF}$, then the effect of the LO phase noise is completely suppressed, so

$$\begin{aligned} v_X(t) = {} & G_L V_{\rm RF}\cos(\omega_{\rm RF}t - \omega_{\rm RF}\tau_L - 2\varphi_m - \varphi_a + \beta \\ & - \tau_{\rm IF}(\omega_{\rm IF} - \omega_n)). \end{aligned} \tag{20}$$

Hence, to have a sustained oscillation, the Barkhausen criterion must be satisfied as

$$\begin{cases} G_L = G_a H_0 C_m V_{\rm ph} V_{\rm LO} J_1(\pi V_{\rm RF}/V_\pi)/V_{\rm RF} = 1 \\ \varphi = \omega_{\rm RF}\tau_L + 2\varphi_m + \varphi_a + \tau_{\rm IF}(\omega_{\rm IF} - \omega_n) \\ \quad = 2k\pi; \quad k = 0, 1, 2, \ldots. \end{cases} \tag{21}$$

It is clear from (21) that the frequency of oscillation is determined by the optical fiber and also by the phase delay due to the other system components such as IF amplifier, mixers, and IF BPF.

The frequency fluctuation and consequently the stability of oscillation frequency is determined by the phase slope of the loop elements, which here is

$$d\varphi/d\omega_{\rm RF} = \tau_L + \tau_{\rm IF} = nL/c + 2Q/\omega_n. \tag{22}$$

A. Phase Noise Analysis

In this subsection, the phase noise analysis of the proposed TF-OEO is presented. Fig. 4 shows a linear time-invariant phase-space model for the proposed TF-OEO, where $\Psi_{\rm amp}(s)$, $\Psi_{\rm mix}(s)$, $\Psi_{\rm opt}(s)$ and $\Phi_{\rm LO}(s)$ are the phase noise of the RF amplifier, RF mixer, microwave photonic link (optical part of Fig. 2), and LO, respectively.

Phase noise of the output oscillation can be expressed as a function of the phase noise of the loop components by applying basic control system theory as

$$\begin{aligned} \Phi(s) = {} & H_1(s)(\Psi_{\rm amp}(s) + \Psi_{\rm mix}(s)) \\ & + H_2(s)(\Psi_{\rm opt}(s) + \Psi_{\rm mix}(s)) + H_3(s)\Phi_{\rm LO}(s) \end{aligned} \tag{23}$$

where $H_1(s)$, $H_2(s)$, and $H_3(s)$ are the phase transfer functions from the RF amplifier, microwave photonic link, and LO to the output, respectively,

$$H_1(s) = 1/(1 - B(s)e^{-s\tau_L}) \tag{24}$$
$$H_2(s) = B(s)/(1 - B(s)e^{-s\tau_L}) \tag{25}$$
$$H_3(s) = (e^{-s\tau_d} - B(s))/(1 - B(s)e^{-s\tau_L}). \tag{26}$$

Using (23)–(26), single-sideband (SSB) phase noise at offset frequency f from the carrier can be expressed as

$$\begin{aligned} L_\varphi(f) = {} & |H_1(j\omega)|^2 S_{\psi_{\text{amp}}}(f)/2 + |H_2(j\omega)|^2 S_{\psi_{\text{opt}}}(f)/2 \\ & + (|H_1(j\omega)|^2 + |H_2(j\omega)|^2) S_{\psi_{\text{mix}}}(f)/2 \\ & + |H_3(j\omega)|^2 S_{\varphi_{\text{LO}}}(f)/2 \end{aligned} \tag{27}$$

where $\omega = 2\pi f$ is the offset angular frequency. For $\omega \ll 1/\tau_L$ and $\omega \ll 1/\tau_{\text{IF}}$ (close-to-carrier phase noise) and assume negligible IF-LO delay mismatch, i.e., $\tau_d \approx \tau_{\text{IF}}$, (27) can be approximated (see the Appendix) as

$$\begin{aligned} L_\varphi(f) = {} & (1 + (f_L/f)^2)(S_{\psi_{\text{amp}}}(f) + S_{\psi_{\text{mix}}}(f))/2 \\ & + (f_L/f)^2 (S_{\psi_{\text{opt}}}(f) + S_{\psi_{\text{mix}}}(f))/2 \end{aligned} \tag{28}$$

where

$$f_L = 1/(2\pi(\tau_L + \tau_{\text{IF}})) = f_{\text{RF}}/2Q_{\text{eq}}. \tag{29}$$

As it is clear from (28) and (29), this model of phase noise is reminiscent of the well-known Leeson's model [63]. Hence, f_L will be the Lesson frequency and the differences are that: 1) here the equivalent quality factor (Q_{eq}) contains the effect of the optical fiber and the IF BPF simultaneously and 2) the noise due to the optical part (high-Q cavity) is also considered in the model.

The noise spectral density of the RF amplifier can be expressed as

$$S_{\psi_{\text{amp}}}(f) = b_0 + b_{-1}/f \tag{30}$$

where $b_0 = Fk_BT_0/P_{\text{RF}}$ is the RF amplifier white noise, F is its noise factor, $k_B = 1.38 \times 10^{-23}$ J/K is Boltzmann's constant, $T_0 = 290$ °K is the ambient temperature, P_{RF} is the oscillation power, and b_{-1} is a constant coefficient that represents the phase flickering of the RF amplifier. Noise spectral density of the RF mixer can also be expressed as (30). The noise spectral density of the microwave photonic link contains three dominant noise sources, laser relative intensity noise (RIN), shot noise, and thermal noise so it can be expressed as

$$S_{\psi_{\text{opt}}}(f) = (k_BT_0 + \langle I_D\rangle^2 N_{\text{rin}} R + 2q\langle I_D\rangle R)/P_{\text{RF}} \tag{31}$$

where $\langle I_D\rangle$ is the average photocurrent, N_{rin} is the laser RIN, and $e = 1.6 \times 10^{-19}$ c is the charge of electron. Fig. 5 shows the predicted phase noise, for the components discussed in the following section (amplifier with phase noise of -110 dBc/Hz at 1 Hz offset frequency, laser with RIN of -125 dBc/Hz at 100 MHz offset frequency, photodetector with a responsivity of 0.4 A/W, IF crystal filter with 3 dB bandwidth of 15 kHz and center frequency of 158.55 MHz and an a 500 m long single-mode optical fiber). As shown in this figure the predicted phase noise is compared with the measured result and with the predicted ultimate phase noise using state-of-the-art components. A more detailed discussion on this figure is found in the following section.

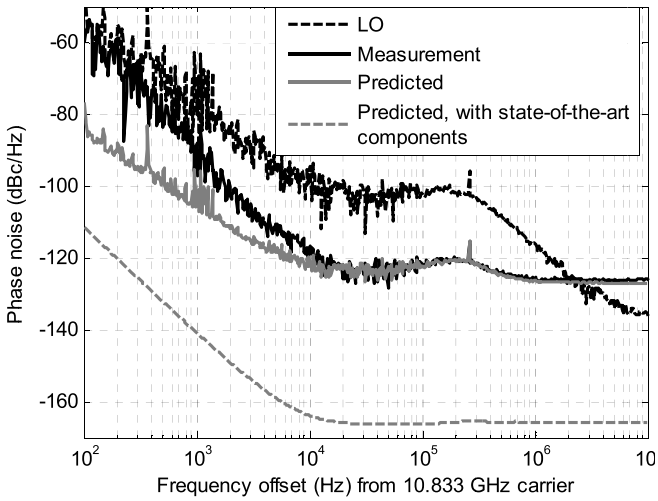

Fig. 5. Phase noise of the output microwave with 10.833 GHz oscillation. Measured phase noise (black solid line), analytical prediction (gray solid line), analytical prediction with the state-of-the-art components (gray dashed line), and measured LO phase noise (black dashed line).

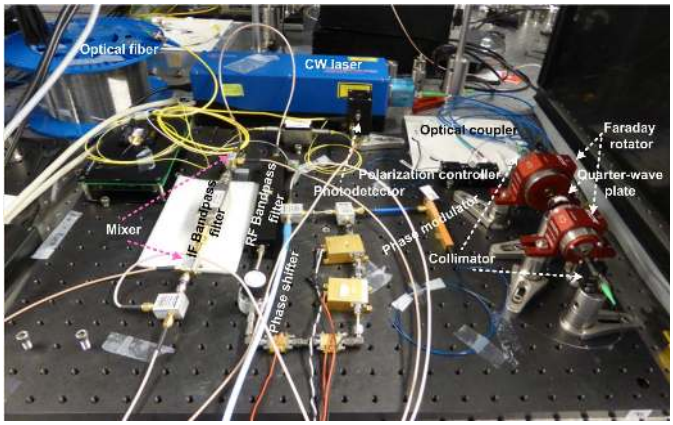

Fig. 6. Photograph of the developed TF-OEO.

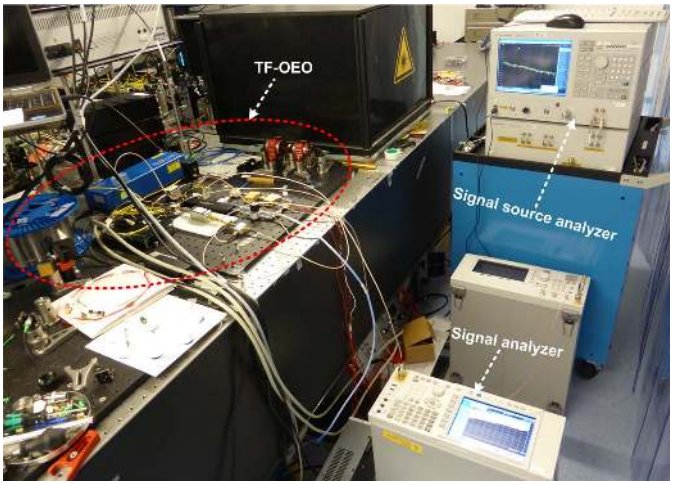

Fig. 7. Photograph of the developed TF-OEO with the measurement equipment.

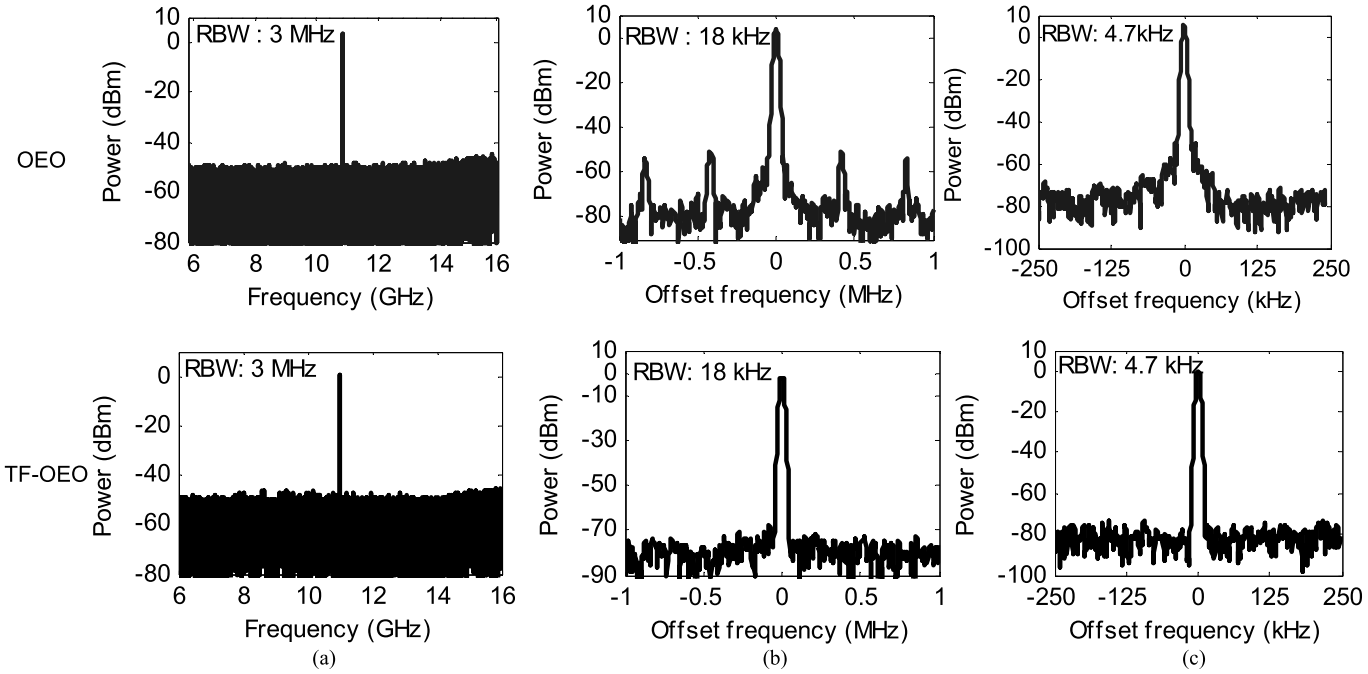

Fig. 8. Measured output spectrum at 10.833 GHz with OEO (top) and TF-OEO (bottom) with a frequency span of (a) 10 GHz, (b) 2 MHz, and (c) 500 kHz. RBW: resolution bandwidth.

IV. Experiment

A setup was performed to measure the performance of the proposed TF-OEO based on the structure shown in Fig. 2. A photograph of the developed TF-OEO is shown in Fig. 6. A continuous-wave light at 1030 nm with 20 dBm power from a laser diode (TOPTICA PHOTONICS DL pro 1040) is sent into the fiber Sagnac loop. An optical isolator (FI-1060-5TI OEM) is used after the laser to avoid back reflections to the optical source. A 20 GHz bandwidth $LiNbO_3$ electrooptic PM was put inside the Sagnac interferometer. The nonreciprocal bias unit is performed in free space using two oppositely oriented 45° faraday rotators (EOT HP-04-R-1030) on both sides of a quarter-wave plate (Thorlabs WPQ05M-1030). The optical delay is provided by a 500 m, single-mode optical fiber. We used a 15 GHz bandwidth InGaAs p-i-n photodiode-based detector (EOT ET-3500F) with a responsivity of approximately 0.4 A/W at 1030 nm. The narrow-band IF crystal filter (from AXTAL) with center frequency of 158.55 MHz and 3 dB bandwidth of 15 kHz has been used. It is worth mentioning here that since we did not have the components at low loss window of optical fiber (1550 nm region) at our laboratory, the experiments were instead performed employing normal components at 1030 nm.

The output electrical spectrum of the TF-OEO is measured by an Agilent N9030A PXA signal analyzer (with the setup shown in Fig. 7) with a span of 10 GHz at 10.833 GHz that is shown in Fig. 8(a) and compared with the output spectrum of the conventional OEO [37]. A focus of the spectrum with a span of 2 MHz and 500 kHz is shown in Fig. 8(b) and (c), respectively. It is clear from these figures that the spurs are completely eliminated and the linewidth is decreased.

The SSB phase noise of the output oscillation is measured by an Agilent E5052B signal source analyzer along with an Agilent E5053A downconverter (with the setup shown in Fig. 7), with the result shown in Fig. 9. As shown in this figure, the phase noise is -120 dBc/Hz at 10 kHz offset frequency from 10.833 GHz carrier. It is clear that the spurs are completely eliminated. The peak around 270 kHz offset frequency is from LO. The phase noise of the TF-OEO is also compared with that of the conventional OEO [37] in this figure. The phase noise is reduced due to the Q-factor enhancement. From (29) the equivalent Q-factor is proportional to the total group delay of the loop. So using (28) and (29) it is obvious that the near-carrier phase noise of a TF-OEO decreases by $20\log((\tau_L+\tau_{\rm IF})/(\tau_L+\tau_{\rm RF}))$, compared to that of a conventional OEO, (where $\tau_{\rm RF}$ is the group delay of the RF BPF inside the loop of the conventional OEO).

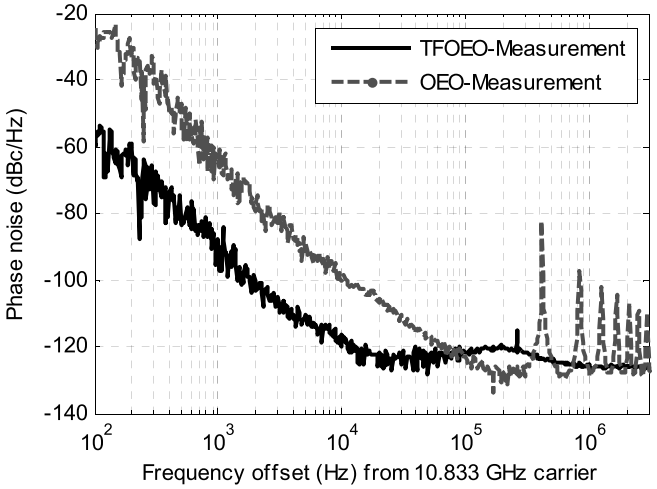

Fig. 9. Phase noise of the output microwave with 10.833 GHz oscillation. OEO (dashed line). TF-OEO (solid line).

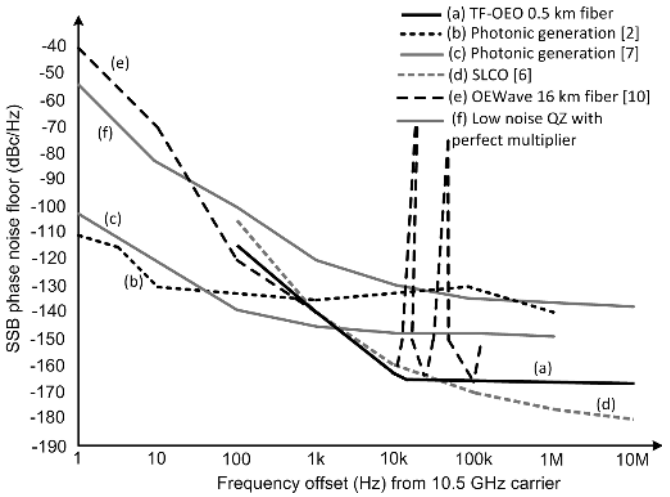

Fig. 10. Phase noise of different types of ultrapure microwave oscillators with an oscillation frequency of 10.5 GHz.

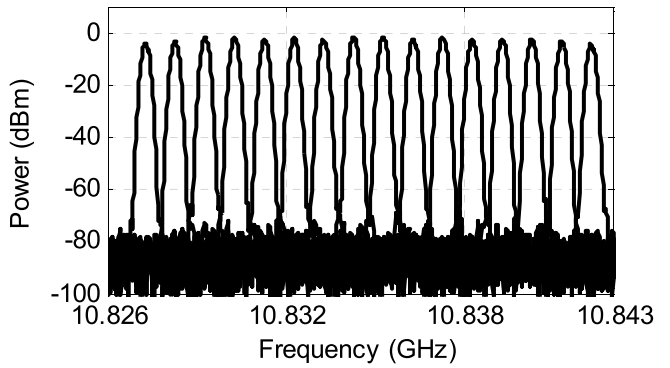

Fig. 11. Measured spectrum of the output microwave at different frequencies with a tuning step of 1 MHz; RBW is 150 kHz.

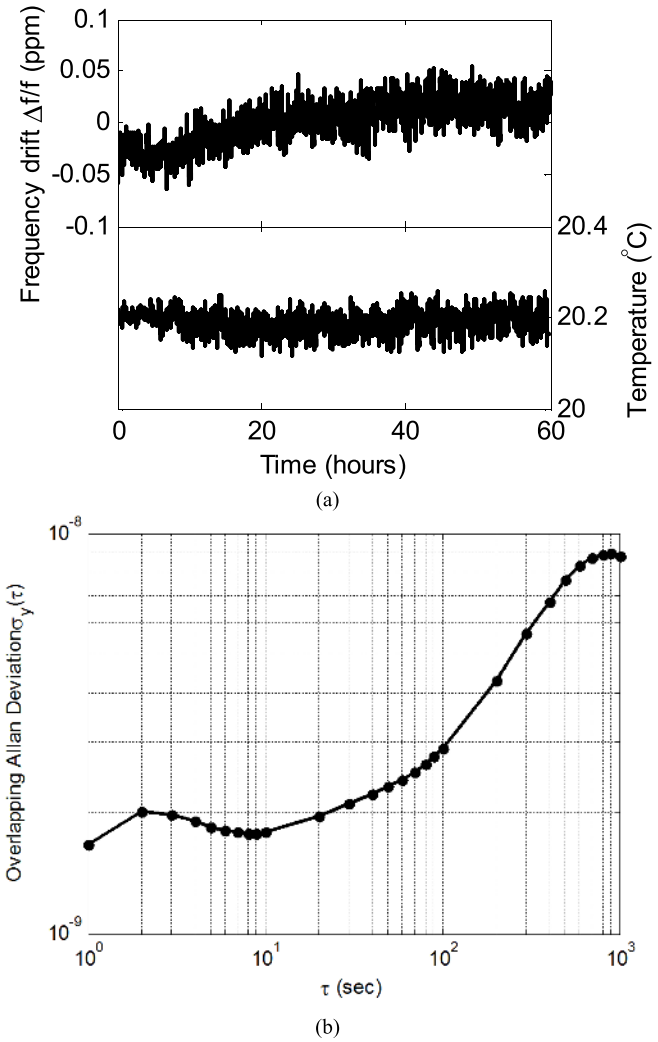

Fig. 12. (a) Long-term frequency drift measurement results over 60 h (±0.05 ppm maximum deviation over 60 hours). (b) Fractional frequency stability (overlapping Allan deviation) based on the measured result in (a).

The phase noise can be more decreased using a few kilometers fiber loop at 1550 nm wavelength and using photodetector, amplifiers, and mixers with lower flicker coefficients and laser with ultralow RIN, but this was not the objective of this paper.

The measured phase noise is also compared with the predicted phase noise, predicted ultimate phase noise using state-of-the-art components, and LO phase noise in Fig. 5. The predicted phase noise is calculated using (27), datasheets of the above discussed components, and measured phase noise of the LO. Below a few kHz offset frequencies, the measured phase noise is poorer than the predicted one, which may be caused due to the flicker noise of the photodetector [64] or AM-to-PM conversion in photodetector [65], and also due to the random-walk and frequency drift induced by environmental factors such as temperature fluctuations and vibration. As shown in this figure, there is a flat noise floor at high offset frequencies (>1 MHz), which is coming from the high frequency noise of the loop components and laser that contains three dominant noise sources, laser RIN, shot noise, and thermal noise. For our TF-OEO, the dominant noise source at high offsets is the RIN of the laser that limits the noise floor of the TF-OEO. Far-from-carrier phase noise of the proposed TF-OEO can be more decreased by employing low noise components.

The following data have also been used for the prediction of the ultimate phase noise using state-of-the-art components (in Fig. 5). Close-to-carrier phase noise of the TF-OEO is limited by the amplifier flicker noise and photodetector AM-to-PM conversion. So, using ultralow phase noise HF/VHF amplifiers (such as API Technologies (formerly SpectrumMicrowave) amplifiers with phase noise of -160 dBc/Hz at an offset of 10 Hz), an ultralow RIN laser (such as Orbits Lightwave Ethernal SlowLight Lasers with -138 dBc/Hz and -165 dBc/Hz at 1 kHz and 100 MHz offset frequencies, respectively) and a photodetector with low power-to-phase conversion factor (such as modified unitraveling carrier (MUTC) photodiodes with $\alpha < 0.1$ rad [65]–[67]), the close-to-carrier phase noise can be reduced tremendously.

It is also clear from (31) that signal-to-noise ratio determines phase noise floor, which is the ratio of the thermal noise, shot noise, and RIN to the microwave power. Besides, for high-power photodetectors, RIN is the dominant source of noise. So, using a high-power photodetector (such as MUTC photodiodes with RF output power of the order

of +14 dBm [66], [67]) and an ultralow RIN laser, phase noise floor can be improved.

The predicted ultimate phase noise using state-of-the-art components of the proposed TF-OEO is compared with those of different classes of ultrapure microwave oscillators in Fig. 10. As shown in this figure, the phase noise of the proposed TF-OEO is comparable to the ultralow phase noise of the state-of-the-art microwave oscillators.

Tunability of the oscillation frequency of the proposed TF-OEO is then investigated. The tuning is realized by tuning the frequency of the LO. The superimposed spectrum of the output microwave oscillation with the frequency tuning within 15 MHz range is shown in Fig. 11. The tuning range is almost the same as the bandwidth of the RF BPF.

The long-term stability is also investigated. To do so, the system is allowed to operate in a room environment for a period of 60 h. Fig. 12(a) shows the measured long-term fractional frequency drift that is ±0.05 ppm maximum fractional frequency deviation over 60 h. The fractional frequency stability (in terms of overlapping Allan deviation [68]) we also calculated using the measured frequency drift, which is shown in Fig. 12(b). This figure shows the drift of 1.6×10^{-9} at 1 s and 8.7×10^{-9} at 1000 s averaging time. The frequency drift of the TF-OEO is limited by the temperature sensitivity of the optical fiber and selection filter which can be improved using a phase lock loop to dynamically compensate the phase fluctuations [14], [44]–[49].

It appears that there will be a tradeoff between phase noise and stability if the fiber length is increased (i.e., phase noise improved, stability reduced). But, using a phase lock loop to dynamically compensate the phase fluctuations [14], [44]–[49] due to the optical fiber length fluctuations, the both phase noise and frequency drift can be improved if the fiber length is increased.

V. Conclusion

In this paper, a novel structure that can realize a bias-drift and spurious free tunable OEO with low phase noise has been presented. It is based on two new structures: 1) a subsystem comprising a Sagnac fiber interferometer, a traveling-wave optical phase modulator, and a nonreciprocal bias unit that function jointly as a bias-drift free amplitude modulator and 2) a TF-LNFA that replaces the RF filtered amplifier. The performances of the proposed TF-OEO were studied by developing a theoretical model. An experiment was performed. Pure microwave oscillations with no spurs are generated. Frequency of the generated microwave oscillation was tuned within 15 MHz range (depends on the bandwidth of the RF BPF). Phase noise of the generated oscillation was −120 dBc/Hz at an offset of 10 kHz from 10.833 GHz carrier, with 36 fs RMS timing jitter integrated from 1 kHz to 10 MHz. The phase noise can be decreased using a fiber with longer length and a laser with ultralow linewidth and RIN. Long-term frequency stability measurement shows ±0.05 ppm maximum deviation over 60 h, which is mostly limited by the drift of the optical fiber delay. The calculated fractional frequency stability (in terms of overlapping Allan deviation) is of the order of 8.7×10^{-9} at 1000 s averaging time. The frequency drift of the proposed TF-OEO can be further decreased by thermal stabilization of the optical fiber delay or using other length stabilization techniques.

Appendix

In this Appendix, the expressions for $|H_1(j\omega)|^2$, $|H_2(j\omega)|^2$ and $|H_3(j\omega)|^2$ are derived that are used in Section III-A. In (13), assuming $\Omega = 0$ (the oscillation frequency falls on the center frequency of the IF BPF) and substituting it into (24) and (25) yields

$$|H_1(f)|^2 = \frac{1 + \omega^2 \tau_{\mathrm{IF}}^2}{2 - 2\cos(\omega\tau_L) + \omega^2 \tau_{\mathrm{IF}}^2 + 2\omega\tau_{\mathrm{IF}} \sin(\omega\tau_L)} \quad (32)$$

$$|H_2(f)|^2 = \frac{1}{2 - 2\cos(\omega\tau_L) + \omega^2 \tau_{\mathrm{IF}}^2 + 2\omega\tau_{\mathrm{IF}} \sin(\omega\tau_L)} \quad (33)$$

where $\omega = 2\pi f$ is the offset angular frequency. For $\omega \ll 1/\tau_L$ and $\omega \ll 1/\tau_{\mathrm{IF}}$ (close-to-carrier phase noise) the following approximation can be used:

$$\sin(\omega\tau_L) \simeq \omega\tau_L, \quad \cos(\omega\tau_L) \simeq 1 - \frac{\omega^2 \tau_L^2}{2}. \quad (34)$$

Substituting (34) into (32) and (33) yields

$$|H_1(f)|^2 = \left(1 + \left(\frac{f_L}{f}\right)^2\right) \quad (35)$$

$$|H_2(f)|^2 = \left(\frac{f_L}{f}\right)^2 \quad (36)$$

where f_L is shown in (29). Assuming negligible IF-LO delay mismatch, i.e., $\tau_d \approx \tau_{\mathrm{IF}}$ and substituting (14) into (26) yields

$$|H_3(f)|^2 \approx 0. \quad (37)$$

Acknowledgment

The authors would like to thank Y. Zhou for his help with the measurements.

References

[1] J. A. Scheer and J. L. Kurtz, *Coherent Radar Performance Estimation*. Norwood, MA, USA: Artech House, 1993.

[2] J. Kim and F. Kärtner, "Attosecond-precision ultrafast photonics," *Laser Photon. Rev.*, vol. 4, no. 3, pp. 432–456, Apr. 2010.

[3] J. Kim, J. A. Cox, J. Chen, and F. X. Kärtner, "Drift-free femtosecond timing synchronization of remote optical and microwave sources," *Nature Photon.*, vol. 2, no. 12, pp. 733–736, Dec. 2008.

[4] E. N. Ivanov and M. E. Tobar, "Low phase-noise sapphire crystal microwave oscillators: Current status," *IEEE Trans. Ultrason., Ferroelect., Freq. Control*, vol. 56, no. 2, pp. 263–269, Feb. 2009.

[5] E. N. Ivanov, D. Mouneyrac, J.-M. L. Floch, M. E. Tobar, and D. Cros, "Precise phase synchronization of a cryogenic microwave oscillator," *Rev. Sci. Instrum.*, vol. 81, no. 6, p. 064702, 2010.

[6] T. M. Fortier *et al.*, "Generation of ultrastable microwaves via optical frequency division," *Nature Photon.*, vol. 5, no. 7, pp. 425–429, Jul. 2011.

[7] X. S. Yao and L. Maleki, "Optoelectronic microwave oscillator," *J. Opt. Soc. Amer. B, Opt. Phys.*, vol. 13, no. 8, pp. 1725–1735, 1996.

[8] A. B. Matsko, D. Eliyahu, and L. Maleki, "Theory of coupled optoelectronic microwave oscillator II: Phase noise," *J. Opt. Soc. Amer. B, Opt. Phys.*, vol. 30, no. 12, pp. 3316–3323, Dec. 2013.

[9] X. S. Yao and L. Maleki, "Multiloop optoelectronic oscillator," *IEEE J. Quantum Electron.*, vol. 36, no. 1, pp. 79–84, Jan. 2000.

[10] J. Yang, Y. Jin-Long, W. Yao-Tian, Z. Li-Tai, and Y. En-Ze, "An optical domain combined dual-loop optoelectronic oscillator," *IEEE Photon. Technol. Lett.*, vol. 19, no. 11, pp. 807–809, Jun. 2007.

[11] E. Shumakher and G. Eisenstein, "A novel multiloop optoelectronic oscillator," *IEEE Photon. Technol. Lett.*, vol. 20, no. 22, pp. 1881–1883, Nov. 15, 2008.

[12] E. Shumakher, "The optoelectronic oscillator: Review and recent advances," in *Proc. IEEE Int. Conf. Microw., Commun., Antennas Electron. Syst. (COMCAS)*, Nov. 2009, pp. 1–5.

[13] X. Liu, W. Pan, X. Zou, B. Luo, L. Yan, and B. Lu, "A reconfigurable optoelectronic oscillator based on cascaded coherence-controllable recirculating delay lines," *Opt. Exp.*, vol. 20, no. 12, pp. 13296–13301, Jun. 2012.

[14] W.-H. Tseng and K.-M. Feng, "Enhancing long-term stability of the optoelectronic oscillator with a probe-injected fiber delay monitoring mechanism," *Opt. Exp.*, vol. 20, no. 2, pp. 1597–1607, Jan. 2012.

[15] R. M. Nguimdo, Y. K. Chembo, P. Colet, and L. Larger, "On the phase noise performance of nonlinear double-loop optoelectronic microwave oscillators," *IEEE J. Quantum Electron.*, vol. 48, no. 11, pp. 1415–1423, Nov. 2012.

[16] M. Shin and P. Kumar, "Optical microwave frequency up-conversion via a frequency-doubling optoelectronic oscillator," *IEEE Photon. Technol. Lett.*, vol. 19, no. 21, pp. 1726–1728, Nov. 1, 2007.

[17] T. Berceli, T. Bánky, and B. Horváth, "Opto-electronic generation of stable and low noise microwave signals," *IEE Proc.-Optoelectron.*, vol. 153, no. 3, pp. 119–127, Jun. 2006.

[18] S. Jia *et al.*, "A novel optoelectronic oscillator based on wavelength multiplexing," *IEEE Photon. Technol. Lett.*, vol. 27, no. 2, pp. 213–216, Jan. 15, 2015.

[19] T. Banky, B. Horvath, and T. Berceli, "Calculations for the measure of the achievable phase noise reduction by the utilization of optimized multiloop opto-electronic oscillators," in *Proc. Eur. Microw. Conf.*, vol. 1. Oct. 2005, p. 4.

[20] W. Zhou and G. Blasche, "Injection-locked dual opto-electronic oscillator with ultra-low phase noise and ultra-low spurious level," *IEEE Trans. Microw. Theory Techn.*, vol. 53, no. 3, pp. 929–933, Mar. 2005.

[21] K.-H. Lee, J.-Y. Kim, and W.-Y. Choi, "Injection-locked hybrid optoelectronic oscillators for single-mode oscillation," *IEEE Photon. Technol. Lett.*, vol. 20, no. 19, pp. 1645–1647, Oct. 1, 2008.

[22] O. Okusaga, W. Zhou, E. Levy, M. Horowitz, G. Carter, and C. Menyuk, "Experimental and simulation study of dual injection-locked OEOs," in *Proc. IEEE Int. Freq. Cont. Symp.*, Apr. 2009, pp. 875–879.

[23] O. Okusaga *et al.*, "Spurious mode reduction in dual injection-locked optoelectronic oscillators," *Opt. Exp.*, vol. 19, no. 7, pp. 5839–5854, 2011.

[24] X. S. Yao, L. Davis, and L. Maleki, "Coupled optoelectronic oscillators for generating both RF signal and optical pulses," *J. Lightw. Technol.*, vol. 18, no. 1, pp. 73–78, Jan. 2000.

[25] C.-J. Lin, Y.-C. Chi, and G.-R. Lin, "Self-starting and overclocking a harmonically mode-locking WRC-FPLD with a dual-loop feedback controller for 10 Gb s^{-1} pulse-data transmission," *Laser Phys. Lett.*, vol. 10, no. 6, p. 065001, 2013.

[26] C.-J. Lin, Y.-C. Chi, and G.-R. Lin, "The self-started 10 GHz harmonic mode-locking of a hybrid weak-resonant-cavity laser diode and fiber ring link," *Laser Phys. Lett.*, vol. 10, no. 6, 2013, Art. no. 065801.

[27] C.-J. Lin and G.-R. Lin, "Frequency chirp and mode partition induced mutual constraint on the side-band phase noise of a mode-locking WRC-FPLD fiber ring self-started with a lengthened feedback loop," *Laser Phys. Lett.*, vol. 23, no. 4, p. 045103, 2013.

[28] J. Marti, F. Ramo, V. Polo, M. Fuster, and J. L. Corral, "Millimeter-wave signal generation and harmonic upconversion through PM-IM conversion in chirped fiber gratings," *Fiber Integr. Opt.*, vol. 19, no. 2, pp. 187–198, 2000.

[29] G. Qi, J. Yao, J. Seregelyi, S. Paquet, and C. Belisle, "Optical generation and distribution of continuously tunable millimeter-wave signals using an optical phase modulator," *J. Lightw. Technol.*, vol. 23, no. 9, pp. 2687–2695, Sep. 2005.

[30] T. Sakamoto, T. Kawanishi, and M. Izutsu, "Optoelectronic oscillator employing reciprocating optical modulator for millimetre-wave generation," *Electron. Lett.*, vol. 43, no. 19, pp. 1031–1033, Sep. 2007.

[31] H. Chi, X. Zou, and J. Yao, "Analytical models for phase-modulation-based microwave photonic systems with phase modulation to intensity modulation conversion using a dispersive device," *J. Lightw. Technol.*, vol. 27, no. 5, pp. 511–521, Mar. 2009.

[32] W. Li and J. Yao, "An optically tunable optoelectronic oscillator," *J. Lightw. Technol.*, vol. 28, no. 18, pp. 2640–2645, Sep. 2010.

[33] W. Li and J. Yao, "An optically tunable frequency-doubling optoelectronic oscillator incorporating a phase-shifted-fiber-Bragg-grating-based frequency-tunable photonic microwave filter," in *Proc. IEEE Microw. Photon. Conf.*, Singapore, Oct. 2011, pp. 429–432.

[34] W. Li and J. P. Yao, "A wideband frequency tunable optoelectronic oscillator incorporating a tunable microwave photonic filter based on phase-modulation to intensity-modulation conversion using a phase-shifted fiber Bragg grating," *IEEE Trans. Microw. Theory Techn.*, vol. 60, no. 6, pp. 1735–1742, Jun. 2012.

[35] B. Yang, X. Jin, X. Zhang, S. Zheng, H. Chi, and Y. Wang, "A wideband frequency-tunable optoelectronic oscillator based on a narrowband phase-shifted FBG and wavelength tuning of laser," *IEEE Photon. Technol. Lett.*, vol. 24, no. 1, pp. 73–75, Jan. 1, 2012.

[36] Z. Tang *et al.*, "Tunable optoelectronic oscillator based on a polarization modulator and a chirped FBG," *IEEE Photon. Technol. Lett.*, vol. 24, no. 17, pp. 1487–1489, Sep. 1, 2012.

[37] S. E. Hosseini, A. Banai, and F. X. Kärtner, "Low-drift optoelectronic oscillator based on a phase modulator in a sagnac loop," *IEEE Trans. Microw. Theory Techn.*, to be published.

[38] L. Maleki and A. B. Matsko, "Optical generation of microwave reference frequencies," in *Proc. 30th URSI General Assembly Sci. Symp.*, Aug. 2011, pp. 1–4.

[39] D. Eliyahu and L. Maleki, "Low Phase noise and spurious level in multi-loop opto-electronic oscillators," in *Proc. IEEE Int. Freq. Control Symp. PDA Exhibit. Jointly 17th Eur. Freq. Time Forum*, May 2003, pp. 405–410.

[40] W. Loh *et al.*, "Amplifier-free slab-coupled optical waveguide optoelectronic oscillator systems," *Opt. Exp.*, vol. 20, no. 17, pp. 19589–19598, Aug. 2012.

[41] D. Eliyahu and L. Maleki, "Tunable, ultra-low phase noise YIG based opto-electronic oscillator," in *IEEE MTT-S Int. Microw. Symp. Dig.*, vol. 3. Jun. 2003, pp. 2185–2187.

[42] D. Eliyahu, K. Sariri, M. Kamran, and M. Tokhmakhian, "Improving short and long term frequency stability of the opto-electronic oscillator," in *Proc. IEEE Int. Freq. Control Symp. PDA Exhibit.*, New Orleans, LA, USA, May 2002, pp. 580–583.

[43] E. J. Adles *et al.*, "Loop-length dependent sources of phase noise in optoelectronic oscillators," in *Proc. IEEE Int. Freq. Control Symp.*, Jun. 2010, pp. 550–553.

[44] A. Docherty, O. Okusaga, C. R. Menyuk, W. Zhou, and G. M. Carter, "Theoretical investigation of optical fiber-length-dependent phase noise in opto-electronic oscillators," in *Proc. IEEE Int. Freq. Control Eur. Freq. Time Forum (FCS)*, May 2011, pp. 1–6.

[45] Y. Zhang, D. Hou, and J. Zhao, "Long-term frequency stabilization of an optoelectronic oscillator using phase-locked loop," *J. Lightw. Technol.*, vol. 32, no. 13, pp. 2408–2414, Jul. 1, 2014.

[46] L. Bogataj, M. Vidmar, and B. Batagelj, "A feedback control loop for frequency stabilization in an opto-electronic oscillator," *J. Lightw. Technol.*, vol. 32, no. 20, pp. 3690–3694, Oct. 2014.

[47] M. Bagnell, J. Davila-Rodriguez, and P. J. Delfyett, "Millimeter-wave generation in an optoelectronic oscillator using an ultrahigh finesse etalon as a photonic filter," *J. Lightw. Technol.*, vol. 32, no. 6, pp. 1063–1067, Mar. 2014.

[48] K. Xu *et al.*, "Long-term stability improvement of tunable optoelectronic oscillator using dynamic feedback compensation," *Opt. Exp.*, vol. 23, no. 10, pp. 12935–12941, May 2015.

[49] T. Bánky, T. Berceli, and B. Horváth, "Improving the frequency stability and phase noise of opto-electronic oscillators by harmonic feedback," in *IEEE MTT-S Int. Microw. Symp. Dig.*, vol. 1. Fort Worth, TX, USA, Jun. 2004, pp. 291–294.

[50] J. K. A. Everard, "A review of low noise oscillator theory and design," in *Proc. IEEE Int. Freq. Symp.*, May 1997, pp. 909–918.

[51] C. McNeilage, E. N. Ivanov, P. R. Stockwell, and J. H. Searls, "Review of feedback and feedforward noise reduction techniques," in *Proc. IEEE Freq. Control Symp.*, May 1998, pp. 146–155.

[52] H. Siedel, "A microwave feed-forward experiment," *Bell Labs Tech. J.*, vol. 50, no. 9, pp. 2879–2916, Nov. 1971.

[53] M. M. Driscoll and R. W. Weinert, "Spectral performance of sapphire dielectric resonator-controlled oscillators operating in the 80 K to 275 K temperature range," in *Proc. 49th IEEE Int. Freq. Control Symp.*, May 1995, pp. 401–412.

[54] E. Rubiola, *Phase Noise and Frequency Stability in Oscillators*. Cambridge, U.K.: Cambridge Univ. Press, 2009.

[55] J. K. A. Everard and M. A. Page-Jones, "Ultra low noise microwave oscillators with low residual flicker noise," in *IEEE MTT-S Int. Microw. Symp. Dig.*, vol. 2. May 1995, pp. 693–696.

[56] J. K. A. Everard and C. D. Broomfield, "Reduced transposed flicker noise in microwave oscillators using GaAs-based feedforward amplifiers," *IEEE Trans. Ultrason., Ferroelect., Freq. Control*, vol. 54, no. 6, pp. 1108–1117, Jun. 2007.
[57] F. G. Ascarrunz, E. S. Ferre, and F. L. Walls, "Investigations of AM and PM noise in X-band devices," in *Proc. 47th IEEE Int. Freq. Control Symp.*, Jun. 1993, pp. 303–311.
[58] M. M. Driscoll, "Microwave oscillator with loop frequency conversion to and signal amplification at an intermediate frequency," U.S. Patent 5 519 359 A, May 21, 1996.
[59] C. McNeilage, J. H. Searls, E. N. Ivanov, P. R. Stockwell, D. M. Green, and M. Mossamaparast, "A review of sapphire whispering gallery-mode oscillators including technical progress and future potential of the technology," in *Proc. IEEE 50th Int. Freq. Control Symp. Expo.*, Montreal, QC, Canada, Aug. 2004, pp. 210–218.
[60] M. A. Page-Jones and J. K. A. Everard, "Enhanced transposed gain microwave oscillators," in *Proc. Eur. Freq. Time Forum*, Brighton, U.K., Mar. 1996, pp. 275–278.
[61] Y. K. Chembo, L. Larger, R. Bendoula, and P. Colet, "Effects of gain and bandwidth on the multimode behavior of optoelectronic microwave oscillators," *Opt. Exp.*, vol. 16, no. 12, pp. 9067–9072, 2008.
[62] F. W. J. Olver, "Bessel functions of integer order," in *Handbook of Mathematical Functions*, M. Abramowitz and I. A. Stegan, Eds. Washington, DC, USA: United States Department of Commerce, 1972, pp. 355–434.
[63] S. E. Hosseini and A. Banai, "Theoretical investigation of the capture effect in intensity-modulation direct-detection microwave photonic links," *Appl. Opt.*, vol. 52, no. 28, pp. 7011–7021, Oct. 2013.
[64] D. B. Leeson, "A simple model of feedback oscillator noise spectrum," *Proc. IEEE*, vol. 54, no. 2, pp. 329–330, Feb. 1966.
[65] E. Rubiola, E. Salik, N. Yu, and L. Maleki, "Flicker noise in high-speed p-i-n photodiodes," *IEEE Trans. Microw. Theory Techn.*, vol. 54, no. 2, pp. 816–820, Feb. 2006.
[66] J. Taylor *et al.*, "Characterization of power-to-phase conversion in high-speed p-i-n photodiodes," *IEEE Photon. J.*, vol. 3, no. 1, pp. 140–151, Feb. 2011.
[67] Z. Li *et al.*, "High-power high-linearity flip-chip bonded modified uni-traveling carrier photodiode," *Opt. Exp.*, vol. 19, no. 26, pp. B385–B390, Dec. 2011.
[68] T. M. Fortier *et al.*, "Photonic microwave generation with high-power photodiodes," *Opt. Lett.*, vol. 38, no. 10, pp. 1712–1714, May 2013.
[69] D. A. Howe, D. W. Allan, and J. A. Barnes, "Properties of signal sources and measurement methods," in *Proc. 4th Annu. Freq. Control Symp.*, May 1981, pp. 669–716.

S. Esmail Hosseini (GS'13) received the B.Sc. degree in electrical engineering from Shiraz University, Shiraz, Iran, in 2007, and the M.Sc. and Ph.D. degrees in electrical engineering from the Sharif University of Technology, Tehran, Iran, in 2009 and 2014, respectively.

From 2013 to 2014, he was a Visiting Scholar with the Center for Free-Electron Laser Science, Deutsches Elektronen-Synchrotron, Hamburg, Germany. Since 2015, he has been a Faculty Member with the Department of Electrical and Computer Engineering, Shiraz University. His current research interests include microwave and millimeter-wave passive and active devices and antennas, microwave photonics, ultrabroad band microwave, ultralow phase noise microwave oscillators, and precision timing distribution and synchronization.

Ali Banai (M'01) was born in Mashhad, Iran, in 1968. He received the B.S., M.S., and Ph.D. degrees in electrical engineering from the Sharif University of Technology, Tehran, Iran, in 1991, 1994, and 1999, respectively.

Since 1999, he has been a Faculty Member with the Department of Electrical Engineering, Sharif University of Technology. His current research interests include nonlinear microwave circuits, the synchronization of coupled oscillators, and numerical techniques in passive microwave circuits.

Dr. Banai was a co-recipient of the Maxwell Premium Award presented at the 2001 Institution of Electrical Engineering, U.K., Microwave, Antennas, and Propagation Proceedings, and the European Microwave Prize in 2015.

Franz X. Kärtner (F'09) is currently the Head of the Ultrafast Optics and X-Rays Group at CFEL-DESY, Hamburg, Germany, and is also a Professor of physics with the University of Hamburg, Hamburg. His current research interests include noise in electronic and optical sources, ultrashort pulse lasers, high-energy subcycle waveform synthesis, frequency combs and precision timing in advanced accelerators and light sources, attosecond physics, and compact free-electron lasers.